J. Fluid Mech. (1998), *vol.* 366, *pp.* 109–133. Printed in the United Kingdom

Exact and approximate solutions to the double-diffusive Marangoni–Bénard problem with cross-diffusive terms

By J. R. L. SKARDA[1], D. JACQMIN[1] AND F. E. McCAUGHAN[2]†

[1] NASA Lewis Research Center, Cleveland, OH 44135, USA

[2] Department of Mechanical and Aerospace Engineering, Case Western Reserve University, Cleveland, OH 44135, USA

(Received for publication 10 June 1997 and in revised form 20 January 1998)

We discuss the linear stability of a cross-doubly-diffusive fluid layer with surface tension variation along the free surface. Two limiting cases of the mass flux basic state are considered in the presence of non-zero Soret and Dufour diffusivities. The first case, which has remained largely unexplored, is one where a temperature difference, $\Delta\bar{T}$, and a concentration difference, $\Delta\bar{C}$, are both imposed across the layer. The second case, which has greater significance to thermosolutal systems, is that where the imposed $\Delta\bar{T}$ across the layer induces a $\Delta\bar{C}$. We rescale the problem in the absence of buoyancy, which leads to a more concise representation of neutral stability results in and near the limit of zero gravity. We obtain exact solutions for stationary stability in both cases. One important consequence of the exact solutions is the validation of recently published numerical results in the limit of zero gravity. Moreover, the precise location of asymptotes in relevant parameter (Sm_c, Ma_c) space are computed from exact solutions. Both numerical and exact solutions are used to further examine stability behaviour. We also derive algebraic expressions for stationary stability, oscillatory stability, frequency, and codimension two point from a one-term Galerkin approximation. The one-term solutions qualitatively reflect the stability behaviour of the system over the parameter ranges in our investigation. A practical consequence is that the nature of the stability (oscillatory or stationary) for a given set of parameter values can be determined approximately, without solving the numerical eigenvalue problem.

1. Introduction

In two-component systems, the gradient of one component often establishes or contributes to a flux of the other component. Such diffusion transport processes are commonly referred to as cross-diffusion. A temperature gradient that forces a concentration gradient in a binary fluid is an example of cross-diffusion also known as the Soret effect. Cross-diffusion is also observed in ternary systems, or isothermal systems with coupled diffusion between the solvent and two solutes. Occasionally both cross-diffusive terms are retained in ternary systems because flux contributions from the gradient of each component is significant. Intensive experimental and theoretical investigation of binary fluid convection has recently been stimulated by microgravity applications such as containerless processing and semiconductor crystal growing. The study of cross-diffusion has also been motivated by its importance to macromolecular

† Present address: Tribune Corporation, Chicago, IL 60611, USA.

polymers, species separation processes, terrestrial materials processing, and oceanography (McDougall 1983; Henry 1990; Legros *et al.* 1990).

Hurle & Jakeman (1969, 1971) observed that small amounts of solute present in thermosolutal systems such as crystal growth melts give rise to convective instabilities. These observations and the ensuing analysis confirmed the important role that the 'Soret effect' plays in establishing instabilities of certain binary-fluid systems in the presence of buoyancy (Platten & Chavepeyer 1973; Henry & Roux 1988; Henry 1990; Jacqmin 1990).

From microgravity processes with free surfaces such as float zone crystal growth techniques, surface tension variations along the free surfaces augment and typically replace buoyancy as the source of the convective instability. In connection with such low-gravity applications, Chen & Chen (1994) recently conducted an extensive numerical study of the stability of an unbounded binary fluid layer in the presence of both buoyancy and surface tension variations along the free surface. A basic state is assumed where the imposed temperature gradient across the layer induces a concentration gradient. This problem was originally studied by Castillo & Velarde (1978), with coupled thermal and solutal buoyancy terms while leaving the surface tension terms uncoupled. (The thermal and solutal Marangoni numbers remain independent when the surface tension variations are uncoupled.) Chen & Chen (1994) recognized that thermal and solutal effects are coupled for both buoyancy and surface tension terms when the applied temperature gradient induces a concentration gradient across the fluid layer. Stability behaviour for a comprehensive set of parameter values is explored in their analysis which also includes the zero gravity limit.

Finger formation in polymer solutions motivated McDougall (1983) to examine the cross-diffusive Rayleigh–Bénard problem for a fluid layer where temperature and concentration gradients are both imposed across the layer. McDougall extended Stern's stability analysis of thermohaline convection (1960) to include both cross-diffusive coefficients. Shear-free boundaries were applied yielding an exact solution to the cross-diffusive problem in the presence of buoyancy. A second study reporting results with temperature and concentration gradients applied across a fluid layer is that of Torrones & Chen (1993). Both basic states, induced concentration gradient and applied concentration gradient are considered in their investigation of a gravity-modulated cross-diffusive fluid layer.

In this paper, the onset of convection due to surface tension variations for an unbounded double diffuse fluid layer is examined. Both cross-diffusive terms are retained in the analysis and two limiting cases of the basic state mass flux are considered. In the first case, a temperature difference, $\Delta\bar{T}$, and a concentration difference, $\Delta\bar{C}$, are both imposed across the fluid layer. This basic state is similar to the buoyancy induced instability studied by McDougall (1983) in connection with ternary systems. The second case which has greater significance to thermosolutal systems is that where the imposed $\Delta\bar{T}$ across the layer induces a $\Delta\bar{C}$. Chen & Chen (1994) have partially explored this limit as part of their combined buoyancy and surface tension stability analysis. We rescale the problem in the absence of buoyancy, which leads to a more concise representation of neutral stability results in and near the limit of zero gravity. More significantly, exact solutions for stationary stability are derived in both cases. One important consequence of the exact solutions is the validation of recently published numerical results in the limit of zero gravity. Moreover, the precise location of asymptotes in relevant parameter (Sm_c, Ma_c) space are computed from exact solutions. The effects of finite disturbance heat and mass transfer from the free surface on stationary stability are also explored with the exact solutions. An interesting

observation is that the expression defining the asymptote for an insulated and an impermeable free surface reduces to the identical form reported by Hurle & Jakeman (1971) for the buoyancy problem when free boundaries are invoked.

We focus on the thermosolutal problem where the Soret effect is often important and the other cross-diffusive term, the Dufour term, is negligible. For both basic states described above, the influence of the Soret diffusion term on the system stability is investigated over a broad range of parameter values. The effect of thermal diffusion on stability boundaries in the more familiar (Ms_c, Ma_c) space is also examined for the standard Soret diffusion system reported in the literature (water–methanol; Hurle & Jakeman 1971). Although emphasis is given to thermosolutal systems, a ternary system (KCl–NaCl–water) where both cross-diffusive coefficients are non-zero is considered briefly.

Linear stability behaviour of double diffusive systems has typically been examined through an extensive set of graphical results that are generated by the numerical solution of the eigenvalue problem. An alternative approach is that of exploiting one-term Galerkin expansions to obtain approximate algebraic expressions that characterize the double diffusive layer stability. Such one-term approaches were advocated by Finlayson (1972) who also demonstrated their applicability for the singly diffusive Rayleigh–Bénard and Marangoni–Bénard problems. Gershuni & Zhukhovitskii (1976) illustrated the use of one-term Galerkin solutions for several variations of the Rayleigh–Bénard problem, although the accuracy of these models is not discussed. We employ a one-term Galerkin formulation to derive explicit relations for predicting stationary stability, oscillatory stability, frequency, and location of the codimension two point. Results from exact and higher-order numerical solutions are used to assess the accuracy and usefulness of the derived algebraic expressions. A comparison of the Galerkin one-term basis functions to the exact and higher-order numerical eigenvectors is also presented.

2. Governing equations

We consider the unbounded cross-doubly-diffusive fluid layer with dimension $0 \leqslant x_3 \leqslant d$. Buoyancy is neglected, and onset of convection due to surface tension variation is examined. The basic state differentiates the two cases of the cross-diffusion we will investigate. For the case when temperature and concentration profiles are imposed, the velocity, temperature, and concentration basic state profiles are:

$$\bar{U} = 0, \quad \bar{T}(x_3) = \bar{T}(0) - \Delta\bar{T}\frac{x_3}{d}, \quad \bar{C}(x_3) = \bar{C}(0) - \Delta\bar{C}\frac{x_3}{d}.$$

Difference quantities of the form $\Delta\bar{y}$ are defined as $\Delta\bar{y} = \bar{y}(0) - \bar{y}(d)$. In the case of Soret diffusion, the applied temperature difference across the layer establishes a concentration gradient, thus the base concentration difference in this case becomes:

$$\Delta\bar{C} = -\frac{D_{21}}{D_{22}}\Delta\bar{T}.$$

The linearized disturbance equations are

$$\frac{\partial}{\partial t}\left(\frac{\partial^2 u_3}{\partial x_j \partial x_j}\right) = \nu \frac{\partial^4 u_3}{\partial x_i \partial x_i \partial x_j \partial x_j}, \tag{1}$$

$$\frac{\partial \theta}{\partial t} = D_{11}\frac{\partial^2 \theta}{\partial x_j \partial x_j} + D_{12}\frac{\partial^2 c}{\partial x_j \partial x_j} + \frac{\Delta\bar{T}}{d}u_3, \tag{2}$$

$$\frac{\partial c}{\partial t} = D_{21}\frac{\partial^2\theta}{\partial x_j\,\partial x_j} + D_{22}\frac{\partial^2 c}{\partial x_j\,\partial x_j} + \frac{\Delta\bar{C}}{d}u_3, \tag{3}$$

where $i,j = 1,2,3$; and u_i, θ and c are the perturbation variables for velocity, temperature, and concentration, respectively. The kinematic viscosity, ν, and diffusivity elements, D_{mn}, are assumed constants. The lower surface at $x_3 = 0$ is rigid ($u_j(0) = 0$), conductive ($\theta(0) = 0$), and permeable ($c(0) = 0$). The upper surface at $x_3 = d$ is free and non-deforming, yielding

$$u_3 = 0, \quad \mu\left(\frac{\partial u_3}{\partial x_k} + \frac{\partial u_k}{\partial x_3}\right) = -\gamma_1\frac{\partial\theta}{\partial x_k} - \gamma_2\frac{\partial c}{\partial x_k}, \tag{4a,b}$$

where $k = 1, 2$ and μ is the dynamic viscosity with constant value. Equation (4*b*) is the disturbance tangential stress condition in the x_1 and x_2 directions at the free surface. Surface tension, σ, is approximated as a linearized function of the diffusion components, T and C, $\sigma = \sigma_0 - \gamma_1(T-\bar{T}) - \gamma_2(C-\bar{C})$. The surface tension variation with temperature, γ_1, and the surface tension variation with concentration, γ_2, are defined as $\gamma_1 = -(\partial\sigma/\partial T)_{C,P}$ and $\gamma_2 = -(\partial\sigma/\partial C)_{T,P}$, respectively (Adamson 1982).

Consideration of heat and mass transfer from the free surface to the environment establishes the remaining two boundary conditions imposed on equations (2) and (3). Continuity of heat and mass transfer across the upper surface leads to

$$\rho c_p\left(-D_{11}\frac{\partial\theta}{\partial x_3} - D_{12}\frac{\partial c}{\partial x_3}\right) = h\theta, \tag{5a}$$

$$-D_{21}\frac{\partial\theta}{\partial x_3} - D_{22}\frac{\partial c}{\partial x_3} = h_s c \tag{5b}$$

2.1. *Imposed temperature and concentration gradients*

When both temperature and concentration gradients are imposed, reference values for length, velocity, time, temperature, and concentration are chosen as:

$$d, \quad \frac{D_{11}}{d}, \quad \frac{d^2}{D_{11}}, \quad \frac{D_{11}\mu}{\gamma_1 d}, \quad \frac{D_{11}\mu}{\gamma_2 d}.$$

The resulting non-dimensional parameters are Prandtl number, *Pr*, diffusivity ratio, τ, Dufour coefficients, *Dm*, Soret coefficient, *Sm*, Marangoni number, *Ma*, solutal Marangoni number, *Ms*, surface Nusselt number, *Nu*, and surface Sherwood number, *Sh*, as defined below:

$$Pr = \frac{\nu}{D_{11}}, \quad \tau = \frac{D_{22}}{D_{11}}, \quad Dm = \frac{D_{12}}{D_{11}}\frac{\gamma_1}{\gamma_2}, \quad Sm = \frac{D_{21}}{D_{22}}\frac{\gamma_2}{\gamma_1},$$

$$Ma = \frac{\gamma_1 d\,\Delta T}{D_{11}\mu}, \quad Ms = \frac{\gamma_2 d\,\Delta C}{D_{22}\mu}, \quad Nu = \frac{hd}{\rho c_p D_{11}}, \quad Sh = \frac{h_s d}{D_{22}}.$$

Alternatively, the commonly chosen temperature and concentration reference values, $\Delta\bar{T}$ and $\Delta\bar{C}$, lead to the ratio of these differences also appearing in the dimensionless cross-diffusive terms, as in the cross-diffusive Rayleigh–Bénard study by McDougall (1983). Our choice of temperature and concentration reference values restricts the occurrence of $\Delta\bar{T}$ and $\Delta\bar{C}$ to *Ma* and *Ms*, respectively. Therefore stability can be examined in the methodical fashion commonly undertaken, where the remaining dimensionless parameters characterize a given fluid system and thus are

fixed by choice of fluid system, while operating conditions of the system are characterized by Ma and Ms. In the absence of buoyancy, the surface tension Soret coefficient, Sm, and surface tension Dufour coefficient, Dm, naturally arise from the non-dimensionalization. These parameters are analogous to the Soret and Dufour coefficients obtained in the buoyancy problem except that they are based on the ratio, γ_1 and γ_2, rather than the ratio of thermal expansion coefficients, β_1 and β_2. It will become apparent that these are more suitable in the absence of buoyancy than adaptation of the Soret separation ratio used in previous studies (Castillo & Velarde 1978; Chen & Chen 1994).

After non-dimensionalizing the equations, solutions are assumed of the form,

$$(u(x_i, t), \theta(x_i, t), c(x_i, t)) = (w(x_3), \phi(x_3), \chi(x_3)) \exp(\mathrm{i}(\alpha_1 x_1 + \alpha_2 x_2) + \lambda t)$$

and the resulting normal mode equations are given, equations (6), (7) and (8), where $\alpha^2 = \alpha_1^2 + \alpha_2^2$. (The same symbols are used for non-dimensional and dimensional variables.)

$$\lambda(D^2 - \alpha^2) w = Pr(D^2 - \alpha^2)^2 w, \tag{6}$$

$$\lambda\phi = (D^2 - \alpha^2)(\phi + Dm\,\chi) + Ma\,w, \tag{7}$$

$$\frac{\lambda\chi}{\tau} = (D^2 - \alpha^2)(Sm\,\phi + \chi) + Ms\,w. \tag{8}$$

The corresponding normal mode boundary conditions are given below:

$$w(0) = 0, \quad Dw(0) = 0, \quad \phi(0) = 0, \quad \chi(0) = 0. \tag{9a–d}$$

At upper surface, $x_3 = 1$

$$w(1) = 0, \quad -D^2 w = \alpha^2(\phi + \chi), \tag{10a, b}$$

$$D\phi + Dm\,D\chi + Nu\phi = 0, \quad Sm\,D\phi + \tau D\chi + Sh\,\chi = 0. \tag{10c, d}$$

2.2. *Induced concentration gradient* (*Soret problem*)

When concentration gradients are induced by temperature, i.e. Soret diffusion, the reference values for T and C are redefined as $\Delta\bar{T}$ and $-(D_{21}/D_{22})\Delta\bar{T}$ analogues to the buoyancy problem (Hurle & Jakeman 1971). All other reference values and dimensionless parameters remain as previously defined. However, Ms is eliminated from our parameter set when ΔC is induced by ΔT across the fluid layer.

The disturbance equations become:

$$\lambda(D^2 - \alpha^2) w = Pr(D^2 - \alpha^2)^2 w, \tag{11}$$

$$\lambda\phi = (D^2 - \alpha^2)\phi - Sm\,Dm(D^2 - \alpha^2)\chi + Ma\,w, \tag{12}$$

$$\lambda\chi = \tau(-(D^2 - \alpha^2)\phi + (D^2 - \alpha^2)\chi) + Ma\,w. \tag{13}$$

Boundary conditions at the lower surface, equations (9*a*)–(9*c*) as well as (10*c*) at the upper surface remained unchanged. However, non-dimensional forms of the tangential stress balance and the flux conditions at the free surface take the following forms: At the upper surface, $x_3 = 1$

$$w = 0, \quad -D^2 w = \alpha^2(\phi - Sm\,\chi), \tag{14a, b}$$

$$D\phi - Sm\,Dm\,D\chi + Nu\,\phi = 0, \quad -D\phi + D\chi + Sh\,\chi = 0. \tag{14c, d}$$

3. Stationary stability – exact solutions

Stability characteristics are examined in this and following sections for broad ranges of relevant dimensionless parameters. Emphasis is placed on the thermosolutal systems

where the Dufour coefficient, *Dm*, can be neglected, and the remaining non-zero cross-diffusive coefficient is the Soret coefficient, *Sm*. Systems where an applied temperature gradient induces a concentration gradient are considered in §3.2. Such conditions were the focus of the analyses by Hurle & Jakeman (1971), Castillo & Velarde (1978), and Chen & Chen (1994). We consider the case where both gradients are imposed across the fluid layer, analogous to the cross-diffusive-Rayleigh–Bénard problem considered by McDougall (1983).

3.1. *Imposed temperature and concentration gradients*

The stationary stability results, $\lambda = 0$, for the cross-doubly-diffusive Marangoni–Bénard problem are first examined. Solving the problem posed by equations (6)–(10) we obtain the following exact solution for stationary stability when both $\Delta\bar{T}$ and $\Delta\bar{C}$ are imposed:

$$\frac{2\alpha^2 - \alpha\sinh 2\alpha}{\alpha^3\cosh\alpha - (\sinh\alpha)^3}$$

$$-\frac{Ma((1-Sm)\,\alpha\cosh\alpha + Sh\sinh\alpha) + Ms((1-Dm)\,\alpha\cosh\alpha + Nu\sinh\alpha)}{4\{(\alpha\cosh\alpha + Nu\sinh\alpha)\,(\alpha\cosh\alpha + Sh\sinh\alpha) - Sm\,Dm\,\alpha^2\cosh^2\alpha\}} = 0. \quad (15)$$

Setting *Sm* and *Dm* to zero, we recover McTaggart's result for the double-diffusive Marangoni problem with no cross-diffusion. Further inspection of (15) reveals that stationary stability is independent of both *Pr* and τ. When *Dm* is sufficiently small, as arises for typical cross-diffusive-thermosolutal systems such as water-methanol, *Ma* is simply proportional to $(1-Sm)^{-1}$. A less stringent criterion is $Sm\,Dm \quad 1$ which is directly established from the exact solution above. Review of cross-diffusivity values (Cussler 1995) confirms this criterion holds for most cross-diffusive thermosolutal and ternary systems. A second consequence of satisfying this criterion is that the cross-diffusion effects occur only in terms of *Sm* and *Dm* in the numerator of (15).

The effects of *Nu* and *Sh* on stationary stability are investigated in (Ma_c, Ms_c) space shown in figures 1 and 2 for the thermosolutal (water–methanol) and ternary (KCl–NaCl–water) systems, respectively. For the double-diffusive-Marangoni problem with no-cross-diffusion, McTaggart (1983) concluded that larger values of *Nu* and *Sh* lead to greater stability. Our results in figures 1(*a*) and 2(*a*) show that a larger value of *Nu* (*Sh*) is stabilizing when Ma_c (Ms_c) is positive which agrees with McTaggart's conclusion. However, a larger value of *Nu* (*Sh*) is destabilizing when Ma_c (Ms_c) is negative which is counter to McTaggart's conclusion. Setting *Dm* and *Sm* to zero in (15) confirms that our observations apply to the no-cross-diffusion case as well. A physical explanation follows from energy availability/dissipation arguments (Chandrasekhar 1981). For a destabilizing temperature gradient, the limit of a conductive free surface, $Nu \to \infty$, is stabilizing in the usual sense in that the fraction of internal energy available to overcome viscous dissipation is reduced. On the other hand, increasing the surface Nusselt number is destabilizing for the stabilizing temperature gradient. By approaching a conductive boundary, a smaller fraction of the internal energy is available to oppose the destabilizing influence of the imposed concentration gradient. An analogous argument can be made in terms of *Sh* for the mass flux condition.

The cross-diffusive results shown in figures 1(*b*) and 2(*b*) reveal that the critical wavenumber, α_c, is constant for all (Ma_c, Ms_c) when $Nu = Sh = 0$. This is consistent with McTaggart's observations for no cross-diffusive problem. She also notes that α_c increases with increasing *Nu* (for fixed *Sh*). We find this is true so long as Ms_c is

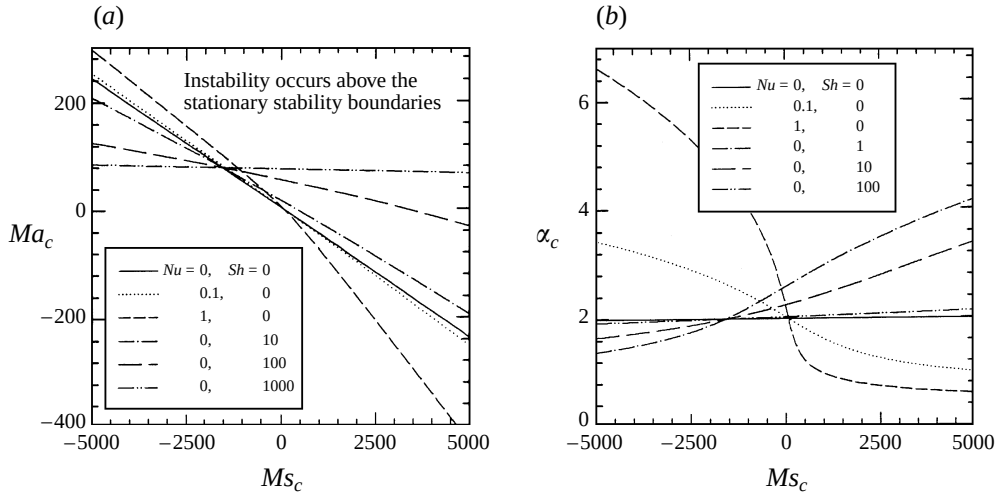

FIGURE 1. Effect of disturbance heat and mass fluxes, *Nu* and *Sh* on stationary stability for a basic state where $\Delta\bar{T}$ and $\Delta\bar{C}$ are both imposed across the layer. (*a*) Ms_c vs. Ma_c for $Sm = -0.0288$ and $Dm = 0$. (*b*) Ms_c vs. α_c for $Sm = -0.0288$ and $Dm = 0$.

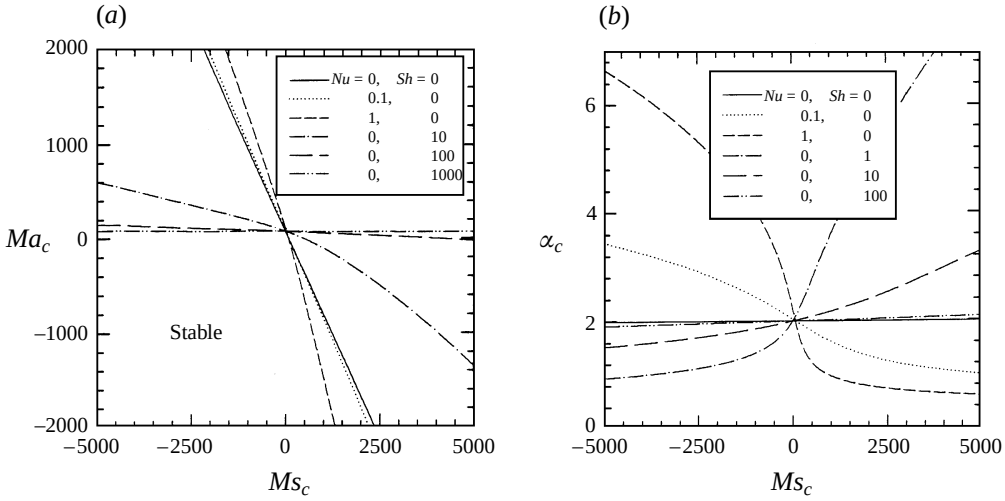

FIGURE 2. Effect of disturbance heat and mass fluxes, *Nu* and *Sh* on stationary stability for a basic state where $\Delta\bar{T}$ and $\Delta\bar{C}$ are both imposed across the layer. (*a*) Ms_c vs. Ma_c for $Sm = 0.072$ and $Dm = 0.183$. (*b*) Ms_c vs. α_c for $Sm = 0.072$ and $Dm = 0.183$.

negative. For increasing Ms_c, figures 1(*b*) and 2(*b*), show that α_c decreases when $Nu > Sh$ and increases when $Nu < Sh$. We also observe that α_c increases (decreases) with *Nu* (*Sh*) for a stabilizing concentration gradient. These effects of *Nu* and *Sh* are reversed for destabilizing concentration gradients. Explanation for the apparent contradictory α_c behaviour is again offered in terms of available energy and dissipation. For increasing *Nu* (*Sh*) the destabilizing temperature (concentration) gradient is driven to larger values, owing to the larger stabilizing concentration (temperature) gradient and *Nu* (*Sh*) values. Therefore, a larger amount of energy is released by surface tension forces and must also be dissipated at neutral stability leading to larger critical wavenumbers. Larger α_c implies that a greater number of smaller sized cells occur along the fluid layer, thereby enhancing dissipation. Somewhat surprisingly, at fixed

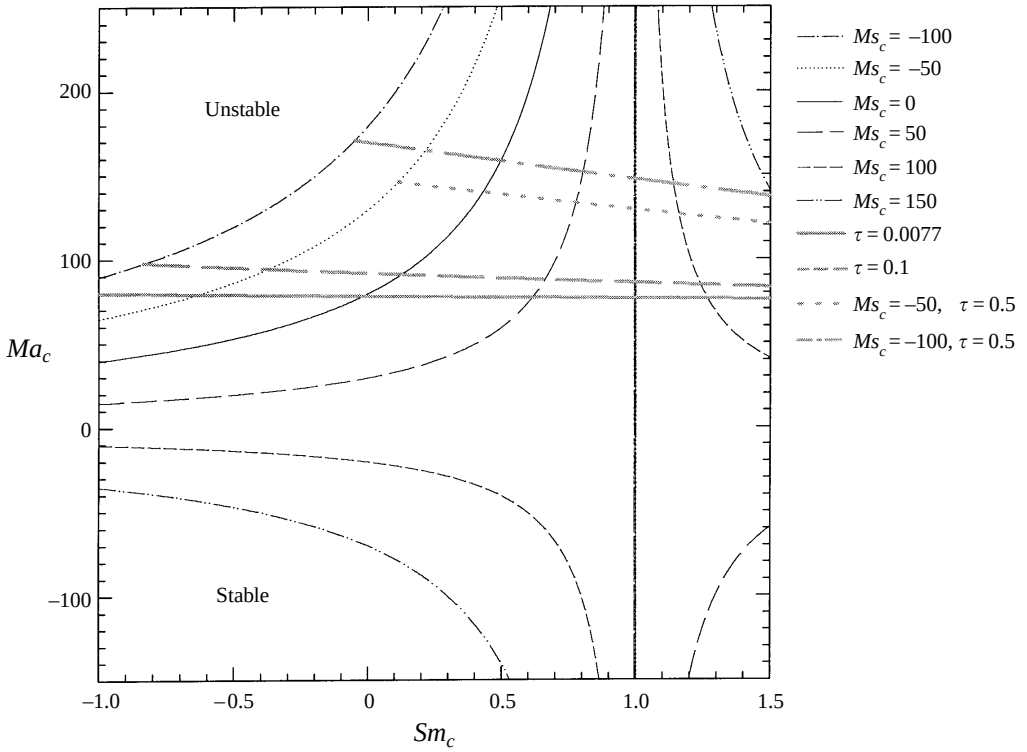

FIGURE 3. Influence of Soret parameter, Sm, on critical Marangoni number, Ma_c. $\Delta\bar{T}$ and $\Delta\bar{C}$ are imposed at boundaries; $Nu = 0$, $Sh = 0$, and $Dm = 0$. Stationary boundaries are thin black lines and oscillatory boundaries are thick grey lines. Oscillatory instability occurs above the oscillatory stability boundaries.

destabilizing concentration gradient (Ms_c), value, α_c decreases with increasing Nu. Apparently, the stabilizing potential of the temperature gradient increases with increasing Nu. This is suggested in figures 1 (*a*) and 2 (*a*) by the decrease in Ma_c for fixed Ms_c values. Therefore, less dissipation is required to offset the energy released by the destabilizing concentration gradient, and this leads to a smaller number of larger cells, i.e. smaller α_c. A similar argument follows for the decrease in α_c associated with increasing Sh values in the presence of stabilizing concentration gradient.

The effect of the Soret diffusion coefficient on neutral stability is shown in figure 3 in terms of Sm for the case of imposed temperature and concentration gradients. Because Dm is negligible in the overwhelming majority of thermosolutal and ternary systems, we set it to zero and neglect the Dufour effect. (A ternary example where both cross-diffusive coefficients are non-zero is briefly studied in §4.1.) The cross-diffusive effects are then completely characterized by Sm and can be compared to the problem where the concentration gradient is induced by the temperature gradient across the layer. Both Nu and Sh are zero and three curves for constant Ms values of -100, 0, 100 are shown in figure 3. While an asymptote is observed at $Sm = 1$, physically realizable systems lie to the left of this value. For this region, increasing values of the Soret parameter, Sm, are stabilizing (destabilizing) for systems with destabilizing (stabilizing) temperature gradients across them. For the present problem, where both temperature and concentration differences are imposed across the layer Ma, Ms and Sm are coupled as $Ms/Ma \propto Sm$. A consequence of this coupling is that Ma must go to zero as $|Sm_c| \to \infty$ for all values of Ms_c.

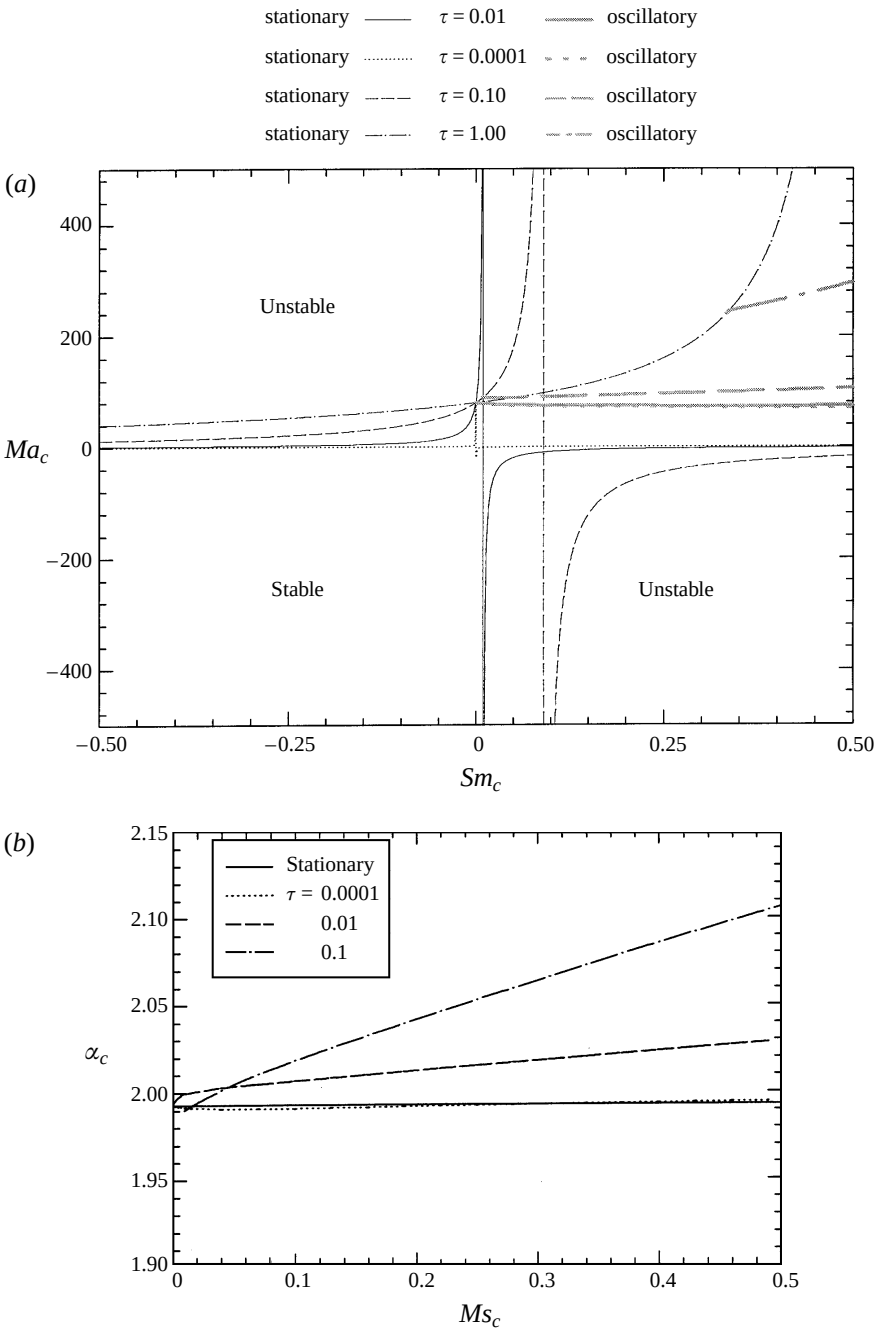

FIGURE 4. Effect of diffusivity ratio, τ, on stability maps in (Sm_c, Ma_c) space. $\Delta\bar{C}$ is induced by applied $\Delta\bar{T}$ for $Dm = 0$, $Nu = 0$, $Sh = 0$. Oscillatory instability occurs above the oscillatory boundaries in the upper right-hand quadrant. (*a*) Sm_c vs. Ma_c. (*b*) Sm_c vs. α_c (for oscillatory boundaries only).

3.2. *Induced concentration gradient* (*Soret problem*)

We now consider stationary stability for the problem where the applied temperature difference across the fluid layer induces a concentration gradient which is commonly referred to a Soret diffusion. The numerical studies of Castillo & Velarde (1978) and

Chen & Chen (1994) assume an insulated free surface, $Nu = 0$, leading directly to the impermeable condition, $Sh = 0$. In both studies, the combined effects of buoyancy and surface tension are treated. By neglecting buoyancy but retaining the more general flux conditions of equations (14*c*) and (14*d*), we obtain the following exact solution for stationary stability of the double diffusive Soret problem. For generality we also retain the Dufour diffusivity term in the energy equation.

$$\frac{Ma \quad Sm\ 1+\dfrac{1-Dm}{\tau}\ -1\ \ \alpha\cosh\alpha+\ \dfrac{Nu}{\tau}Sm-Sh\ \ \sinh\alpha}{2\{(Sm\,Dm-1)\,\alpha^2(1+\cosh 2\alpha)+Nu\,Sh(1-\cosh 2\alpha)-(Nu+Sh)\,\alpha\sinh 2\alpha\}} + \frac{8\alpha^2-4\alpha\sinh 2\alpha}{\sinh 3\alpha-3\sinh\alpha-4\alpha^3\cosh\alpha}=0. \quad (16)$$

Stationary stability results from (16) are shown in figure 4, for different values of τ. The overall behaviour in (Sm_c, Ma_c) space is quite similar to the Rayleigh–Bénard stationary stability results in (Sr_c, Ra_c) space reported by Hurle & Jakeman (1971) where Sr is defined as $D_{21}\beta_2/D_{22}\beta_1$, and Ra is the Rayleigh number defined in the usual manner (Hurle & Jakeman 1971). Asymptotic behaviour occurs at a finite Sm_c value and Ma_c is driven to zero as $|Sm_c| \to \infty$. Chen & Chen (1994) observed this behaviour in their numerical simulations of the surface-tension-induced Soret case. Because of their interest in the combined buoyancy–surface-tension problem, they plotted a family of curves in (Sr_c, Ma_c) space. Each curve was associated with a constant material parameter, K, where $K = \beta_1\gamma_2/\beta_2\gamma_1$. However, we find in the limit of zero gravity that the family of curves collapses to a single curve if the abscissa is replaced with the product, $K\,Sr$ (or Sm in our notation). Results from their figures 5 and 9 reduces to the single curve, $\tau = 0.01$, in our figure 4. While our parameterization works well in the limit of zero gravity. Chen & Chen's material surface, K, or equivalent, is necessary to appropriately tackle the combined buoyancy/surface-tension Soret problem, as was their objective.

The exact location of the asymptote observed in figures 4, 5 and 6 is given by equation (17).

$$Sm_\infty = \frac{\alpha\,\mathrm{cotanh}\,\alpha+Sh}{1+\dfrac{1-Dm}{\tau}\ \ \alpha\,\mathrm{cotanh}\,\alpha+\dfrac{Nu}{\tau}}. \quad (17)$$

For liquid thermosolutal systems the Dufour diffusive contribution can be neglected, $Dm = 0$ (Hurle & Jakeman 1971). If we then consider the flux boundary conditions typically applied to the Soret problem, an insulated and impermeable surface, the location of the asymptote reduces to a simple function of τ, $Sm_\infty = (1+(1/\tau))^{-1}$. This is the identical expression for the asymptote location in (Sr_c, Ra_c) space, $Sr_\infty = (1+(1/\tau))^{-1}$, which Hurle & Jakeman (1971) derived for the case of the buoyancy-induced Soret problem with free–free surfaces.

In our analysis, the species equations of a ternary system are always chosen such that $\tau \leqslant 1$, which is also consistent with thermosolutal systems. For an insulated and impermeable free surface, the location of the asymptote is then bounded on the interval $0 < Sm_\infty \leqslant 0.5$ for $0 < \tau < 1$. For water–alcohol mixtures and liquid metal alloys, typical τ values are 0.01 and 0.0001, respectively; and for such systems, we conclude $Sm_\infty \approx \tau$. In addition to shifting Sm_∞ to the right, the stationary stability curves are shifted away from the abscissa ($Ma_c = 0$), with increasing τ resulting in a stabilizing effect on the stationary stability curves. Chen & Chen (1994) report similar findings in (Sr_c, Ra_c) space for the buoyancy problem at finite Ma values. However, they

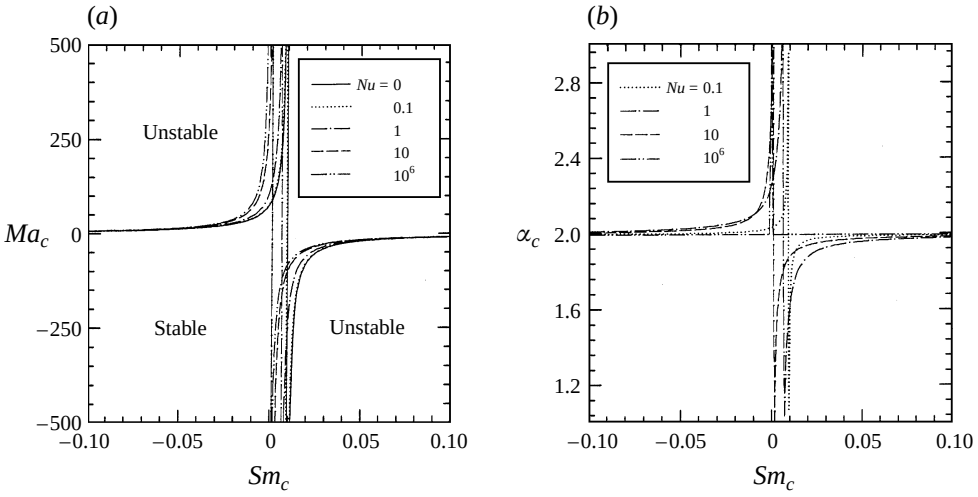

FIGURE 5. Effect of disturbance heat and mass fluxes, *Nu* and *Sh* on stationary stability for a basic state where $\Delta\bar{C}$ is induced by $\Delta\bar{T}$. Impermeable free surface, $Sh = 0$. $\tau = 0.01$, $Dm = 0$, $Sh = 0$. (*a*) Sm_c vs. Ma_c for *Nu* values of 0, 0.1, 1, 10, and 10^6. (*b*) Sm_c vs. α_c for *Nu* values of 0.1, 1, 10, and 10^6.

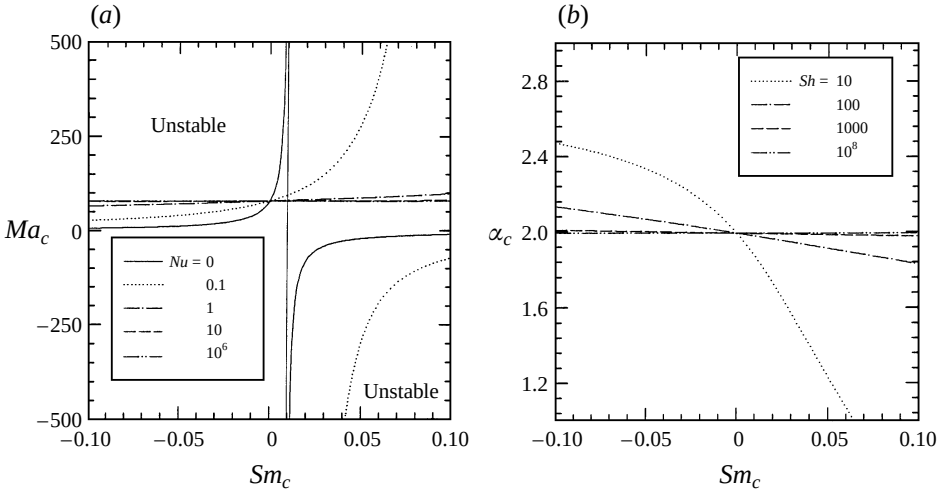

FIGURE 6. Effect of disturbance heat and mass fluxes, *Nu* and *Sh* on stationary stability for a basic state where $\Delta\bar{C}$ is induced by $\Delta\bar{T}$. Insulated free surface, $Nu = 0$, $\tau = 0.01$, $Dm = 0$, $Sh = 0$. (*a*) Sm_c vs. Ma_c for *Sh* values of 0, 10, 100, 1000, and 10^8. (*b*) Sm_c vs. α_c for *Sh* values of 10, 100, 1000 and 10^8.

concluded that decreasing τ (increasing Le; $Le = 1/\tau$ where Le is the Lewis number (Chen & Chen 1994)) is stabilizing in the equivalent of the upper right-hand quadrant our figure 4(*a*). We believe that this inconsistency is due to reference axes and is reconciled as follows. Chen & Chen view the shift of Sm_c to the right as destabilizing, since less of the quadrant area is then stable. However, the more appropriate reference is the asymptote, especially since we can determine it exactly. Thus, our comparisons are made based on the axes, $Ma_c = 0$ and $Sm_c - Sm_\infty$. While the asymptote moves further into the upper right-hand quadrant for larger τ values, the fact that the curves are shifted to larger Ma_c is then stabilizing.

When a free surface with finite conductivity or permeability is considered, Sm_∞ is dependent on α in addition to *Nu* and *Sh*. In the limit of a conducting free surface,

Sh	α_c in $\lim \lvert Sm\rvert \to \infty$
1	2.25
10	2.74
100	2.98
1000	3.01

TABLE 1. Influence of Sh on asymptotic values of α_c in the limit $|Sm| \to \infty$. The concentration gradient is induced by an imposed temperature gradient. ($Nu = 0$, $\tau = 0.01$)

$Nu \to \infty$, equation (17) confirms that $Sm_\infty \to 0$. As already discussed, Sm_∞ lies in the right-hand half-plane, and reaches its maximum value in the limit of an insulated free surface, $Nu = 0$ (for $Sh = 0$). Its exact position is dependent on τ. An increase in Nu then shifts the asymptote leftward toward the ordinate, $Sm = 0$ as observed in figure 5(a). In (Sm_c, Ma_c) space, this leftward displacement is stabilizing (destabilizing) to stationary stability curves associated with destabilizing (stabilizing) temperature gradients (figure 5a). From (17), it also follows that $Sm_\infty \to \infty$ as $Sh \to \infty$, which is observed in figure 6(a). In the sense that the stationary stability curves are displaced upwards for destabilizing temperature gradients, Sh is stabilizing. The surface Sherwood number, Sh, is destabilizing to the right of Sm_∞. However, the upwards or downwards displacement of the stationary stability curves are largely due to the rightward shift of Sm_∞ as Sh increases. We note that for $Sh = 100$, 1000, and 10^8, only portions of curves associated with destabilizing temperature gradients are visible in figure 6(a) since Sm_∞ values lie beyond the range of values shown. In the limit of a permeable free surface, $\chi(1) = 0$, and the problem reduces to the singly diffusive system studied by Pearson (1959).

When the free surface is insulated and impermeable, Pearson's (1959), α_c value, $\alpha_{cp} = 1.9929$, is obtained along the stationary stability curves. However, if Nu or Sh differs from zero, α_c varies along the stationary stability curve as shown in figures 5(b) and 6(b). For varying Nu, and Sm values approaching Sm_∞, the wavenumber increases (decreases) for destabilizing (stabilizing) temperature gradients, while $\alpha_c \to \alpha_{cp}$ as $|Sm| \to \infty$ (figure 5b). Near Sm_∞, larger quantities of energy must be dissipated when the temperature is destabilizing. This is most efficiently accomplished with a larger number of smaller sized cells as noted in the previous section. Conversely, when the induced concentration gradient is destabilizing ($Sm > Sm_\infty$), increasing Nu reinforces the stabilizing potential of the temperature gradient, and reduced dissipation required results in less vorticity and larger flow cells.

For the finite Sh results, in figure 6(b), we find that α_c asymptotically decreases (increases) as $Sm \to Sm_\infty$ for $Sm < Sm_\infty$ ($Sm > Sm_\infty$). When $|Sm_\infty| \to \infty$, α_c asymptotically approaches the values given in table 1. Although table 1 shows that the asymptotic values of α_c increase with larger Sh, the reversed behaviour is observed for $Sm < Sm_\infty$ within the physically realistic range of Sm values shown in figure 6(b). Near Sm_∞, the concentration gradient's potential to absorb the energy released by the destabilizing temperature gradient increases with larger Sh values. Therefore, less viscous dissipation, consequently, less vorticity is required, leading to larger cells. Conversely, a destabilizing induced concentration gradient requires greater dissipation near Sm_∞, leading to more vorticity (smaller α_c). While slight changes in Nu or Sh lead to small shifts in Sm_∞, the wavenumber can deviate greatly from α_{cp} near Sm_∞ with respect to the insulated-impermeable free surface.

4. Onset of oscillatory instability

The time-dependent or oscillatory stability boundaries were computed using a Chebyshev collection scheme. Ten collocation points were typically sufficient to give five- and six-digit agreement with the exact solutions for α_c and Ma_c. Oscillatory results at large Sm_c values and small τ required between 15 and 25 collocation points to achieve five- and six-digit agreement with the next lower-order accurate solution. Seven collocation points provided two- to three-digit agreement in α_c and Ma_c values.

4.1. *Imposed temperature and concentration gradients*

Oscillatory stability boundaries in (Sm_c, Ma_c) space are represented by the thick lines in figure 3. As previously noted, an insulated and impermeable free surface is applied and $Dm = 0$. Starting from the codimension two point, all the oscillatory boundaries in figure 3 decrease with increasing Sm_c. The codimension two point can be viewed as the coalescence point of two neutral modes. This coalescence is the intersection point of the stationary and oscillatory boundaries in figure 3. Stationary solutions occur to one side of the coalescence point, and two oscillatory solutions occur to the other side. For small values of τ, the variation between the constant Ms_c oscillatory branches also become quite small, as is the case for τ values of 0.0077 and 0.1. Three oscillatory stability branches for the constant Ms_c values of 50, -50, and -100 are actually represented along the curves designated by these τ values. Each curve begins at the corresponding codimension two point in table 2 and decreases with increasing Sm_c. When both temperature and concentration differences are imposed across the layer, stationary stability boundaries are independent of τ. In contrast, increasing τ is found to stabilize the time-dependent stability boundaries in figure 3 for all Sm_c values. Ho & Chang (1988) reported the same stabilizing behaviour for their no-cross-diffusion doubly diffusive Marangoni results. The explanation that overstability relies on differences in D_{11} and D_{22}, and opposing gradients of the stability agents, temperature, T, and concentration, C, can be extended to include cross-diffusive terms (Turner 1973; Legros *et al.* 1990). For example, the combination of positive D_{21}, positive $\Delta\bar{T}$, and negative $\Delta\bar{C}$, further retards the diffusion rate of C, therefore reinforcing oscillatory overstability.

Cross-diffusion also leads to changing the nature of the instability. For example, in the absence of cross-diffusion, $Sm = 0$, onset of convection is stationary for Ms_c values of 0 and 50, when $\tau = 0.0077$. However, when Sm values exceed 0.0079 and 0.63, respectively, for the above Ms_c values, oscillatory onset occurs.

The effects of cross-diffusion on the stability boundaries in more typical (Ms_c, Ma_c) space are examined in figure 7 for a thermosolutal system and ternary system. The thermosolutal system is the water–methanol system considered in the buoyancy driven Soret studies of Hurle & Jakeman (1971) and Jacqmin (1998). The ternary system is a KCl–NaCl–water solution where both cross-diffusive coefficients are non-zero (Cussler 1995). Both systems are shown and compared to the equivalent systems in the absence of cross-diffusion, $Sm = 0$ and $Dm = 0$. The codimension two points for these systems are given in table 3.

Differences between the thermosolutal system, $Sm = -0.028$, and no-cross-diffusion, $Sm = 0$ are undetectable in figure 7, although our numerical results reveal that cross-diffusion slightly stabilizes both stationary and oscillatory branches. Comparison of α_c and ω for zero and non-zero Sm in figure 8 also suggests that the effect of the cross-diffusion term ($Sm = -0.028$) is negligible for this particular thermosolutal system. We

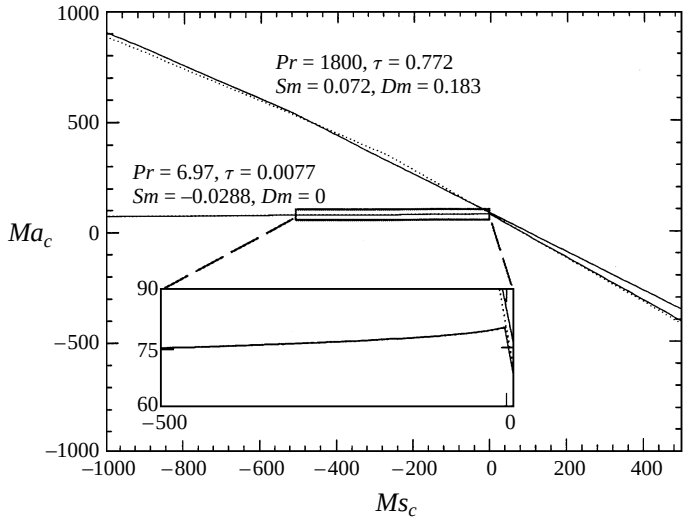

FIGURE 7. Stability maps in (Ms_c, Ma_c) space for $\Delta\bar{T}$ and $\Delta\bar{C}$ both imposed across the fluid layer. Comparisons of stability boundaries for cases ——, with and ....., without cross-diffusive terms are shown for a thermosolutal system, $Pr = 6.97$, $\tau = 0.0077$, $Sm = -0.0288$, $Dm = 0$; and a ternary system, $Pr = 1800$, $\tau = 0.772$, $Sm = 0.072$, and $Dm = 0.183$. Insert shows slight destabilization along the oscillatory branch moving away from the codimension two point.

τ	Ms_{co2}	Sm_{co2}	Ma_{co2}	$Sm_{co2\text{-}1T}$	$Ma_{co2\text{-}1T}$
0.0077	−50	-6.076×10^{-1}	80.62	6.763×10^{-1}	72.52
0.0077	0	7.880×10^{-3}	80.24	7.960×10^{-3}	72.13
0.0077	50	6.251×10^{-1}	78.85	6.995×10^{-1}	71.25
0.1	−100	-8.354×10^{-1}	97.86	-9.273×10^{-1}	89.01
0.1	−50	-3.958×10^{-1}	92.86	-4.469×10^{-1}	84.01
0.1	0	1.080×10^{-1}	89.25	9.427×10^{-2}	79.01
0.5	−100	-5.120×10^{-2}	170.86	-8.000×10^{-2}	158.8
0.5	−50	1.115×10^{-1}	145.86	9.179×10^{-2}	133.8

TABLE 2. Codimension two points corresponding to figure 3. Both temperature and concentration gradients are imposed across the fluid layer. *co*2 denotes spectral and *co*2-1T denotes one-term Galerkin results.

τ	Sm	Dm	Ms_{co2}	Ma_{co2}	$Ms_{co2\text{-}1T}$	$Ma_{co2\text{-}1T}$
0.0077	−0.0288	0	−2.970	80.24	−2.673	72.15
0.0077	0	0	−0.6403	80.23	−0.5786	72.15
0.772	0.072	0.183	−517.7	540.7	−467.9	488.0
0.772	0	0	−269.6	349.2	−242.3	313.9

TABLE 3. Codimension two points corresponding to figure 7. Both temperature and concentration gradients imposed across fluid layer. *co*2 denotes spectral and *co*2-1T denotes one-term Galerkin results.

note that this is contrary to the situation when the concentration gradient is induced by the temperature gradient as considered below in §4.2.

Careful examination of the thermosolutal oscillatory branches in figure 7 reveals that Ma_c gradually decreases in the direction of negative Ms_c. We have also observed this

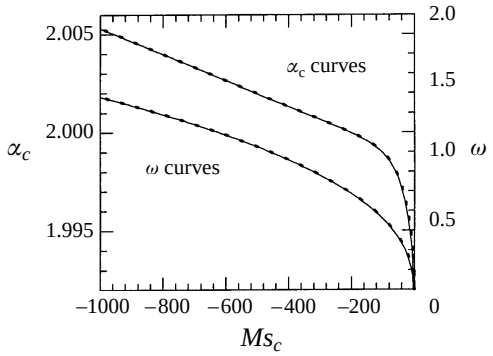

FIGURE 8. Critical wavenumbers, α_c, and frequencies, ω, corresponding to the thermosolutal system in figure 7 are shown. α_c vs. Ms_c and ω vs. Ms_c are shown for cases ——, with and ……, without cross-diffusivity terms for $Pr = 6.97$, $\tau = 0.0077$, $Sm = -0.0288$, $Dm = 0$.

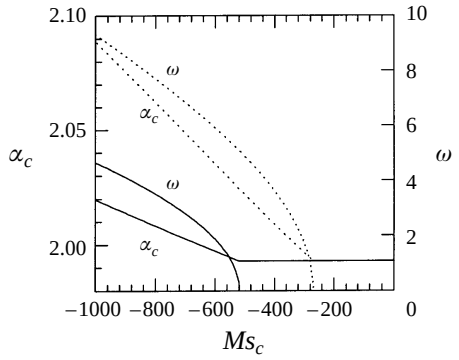

FIGURE 9. Critical wavenumbers, α_c, and frequencies, ω, corresponding to the ternary system in figure 7 are shown. α_c vs. Ms_c and ω vs. Ms_c are shown for cases ——, with and ……, without cross-diffusivity terms $Pr = 1800$, $\tau = 0.772$, $Sm = 0.072$, and $Dm = 0.183$.

destabilizing behaviour at τ (and Pr) values representative of liquid metals. Energy stability results reported by Velarde & Castillo (1982) show a large destabilizing effect associated with decreasing Ms_c whereas the oscillatory boundary from their linear stability results indicate Ma_c is invariant to changes in Ms. Ho & Chang (1988) also show linear stability results for the double-diffusion-Marangoni–Bénard problem at different values of τ. As τ decreases (from 1), the stabilizing effect of increasing Ms_c is reduced; however, their curve for $\tau = 0.0001$ also appears as a horizontal line. Our results show definitively that with or without cross-diffusion, decreasing Ms_c has a stabilizing effect on the oscillatory branch, i.e. Ma_c increases, for moderately small values of τ. However, for small τ values such as 0.01 (water–methanol) or 0.0001 (liquid metals), decreasing Ms_c does not lead directly to the constant value of 79.604 for Ma_c but is slightly destabilizing.

For the ternary system if KCl–NaCl–water, small differences are visible between the stability boundaries, with and without the cross-diffusive terms in figure 7. For this system, the positive Sm value was confirmed to be destabilizing while the positive Dm value is stabilizing, and the combined effect of the cross-diffusive terms is to destabilize both the oscillatory and stationary stability boundaries. The cross-diffusive terms influence the codimension two point more significantly. Figures 7 and 9 reveal that Ms_{co2}, is shifted from a value of -269.6 neglecting cross-diffusion to -517.7 when the cross-diffusive terms are included. Setting Sm to zero with $Dm = 0.183$, we found that

τ	Sm_{co2}	Ma_{co2}	$Sm_{co2\text{-}1T}$	$Ma_{co2\text{-}1T}$
0.0001	1.037×10^{-8}	79.62	1.03×10^{-8}	71.6
0.01	1.026×10^{-4}	80.44	1.03×10^{-4}	72.3
0.1	9.305×10^{-3}	88.68	9.35×10^{-3}	79.8
1	3.370×10^{-1}	244.6	3.38×10^{-1}	220.7

TABLE 4. Codimension two points corresponding to figure 4. Concentration gradient is induced by an imposed temperature gradient

only stationary onset occurred over the full range of Ms_c shown in figure 7, while setting Dm to zero and retaining $Sm = 0.072$ leads to a codimension two point at $Ms_c = -180.2$. In figure 9, the combined effect of the cross-diffusive terms is observed to decrease both α_c and ω values beyond values predicted in the absence of the cross-diffusive terms. These results suggest that the effect of the cross-diffusive terms on the stability boundaries, codimension two point, and ω is one of competition rather than reinforcement when both Sm and Dm are positive. The sensitivity of the codimension two point to both cross-diffusive terms may warrant further investigation in future studies of ternary systems.

4.2. *Induced concentration gradient* (*Soret problem*)

Time-dependent or oscillatory neutral stability boundaries are shown in (Sm_c, Ma_c) space in figure 4(*a*) and dimensionless frequencies are plotted in figure 4(*b*). The Pr value for all results shown in 6.97.

The oscillatory branches begin at the codimension two points given in table 4 and continue rightward with increasing Sm_c. Increasing τ has a stabilizing effect on the oscillatory branches as confirmed by the upward displacement of these branches in figure 4(*a*). We note that even for a τ value of 1, when the characteristic diffusion times of heat and concentration are equal, oscillatory instability is possible in the presence of cross-diffusion. The minimum thermal-diffusion contribution necessary to establish oscillatory instability occurs at the codimension two points of $Sm_c \approx 0.337$ (see table 4). The oscillatory stability boundaries for τ values of 0.1 and 1 are stabilized by increasing Sm_c from the codimension two point, while oscillatory curves for τ values of 0.01 and 0.0001 initially decrease (destabilizing) with Sm_c. For $\tau = 0.01$, increasing Sm_c is found to stabilize the oscillatory boundary beyond an Sm_c value of 0.337. As indicated below, this is consistent with the behaviour reported by Chen & Chen (1994) for $\tau = 0.01$. Although we suspect similar behaviour for the $\tau = 0.0001$ curve, we did not observe an upward turn of this curve while extending our calculations to $Sm_c = 2$ (well beyond Sm_c range for liquid thermosolutal and ternary systems). However, we did find that the oscillatory boundary for $\tau = 0.001$ (not shown in figure 4*a*) reaches a minimum at $Sm_c \approx 1.3$, at which point increasing Sm_c leads to a stabilizing effect.

As part of their combined buoyancy/surface-tension work, Chen & Chen (1994) present a family of oscillatory stability curves in (Sr_c, Ma_c) space for different K values where K and Sr were defined in §3.2. Constant values of Pr and τ were chosen as 7 and 0.01, respectively, for their analysis. For the same reasons as noted in §3.2, the multiple curves in their figures 6 and 8 collapse to the single curve, the $\tau = 0.01$ curve, in each of our figures 4(*a*) and 4(*b*). We again remark that $Sm_c = K\,Sr_c$. This would also explain why only the $K = 1$ curve showed an initially destabilizing and then stabilizing influence of Sr_c on Ma_c while all other curves ($K < 1$) displayed a destabilizing influence. The effect of the smaller K values is to compress the Sr_c range to smaller Sm_c

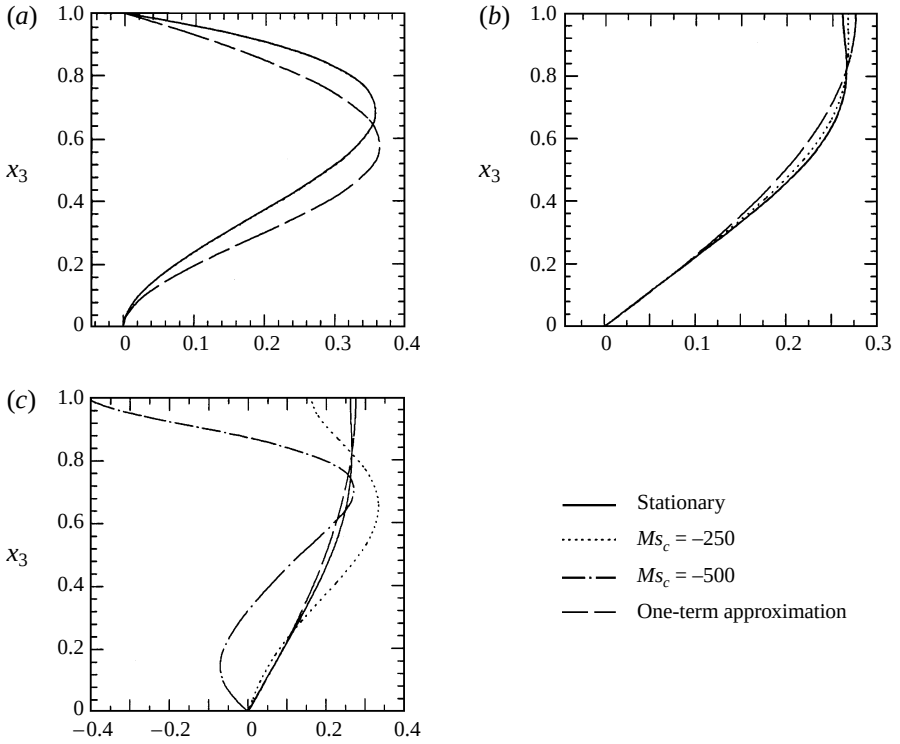

FIGURE 10. Velocity, temperature, and concentration eigenvector profiles at neutral stability. $\Delta\bar{T}$ and $\Delta\bar{C}$ both imposed across the layer. $Pr = 6.97$, $\tau = 0.0077$, $Sm = -0.028$, $Dm = 0$, $Nu = 0$ and $Sh = 0$. (*a*) Normalized velocity eigenvector vs. x_3. (*b*) Normalized temperature eigenvector vs. x_3. (*c*) Normalized concentration eigenvector vs. x_3.

values which are always below the Sm_c minimum of 0.32 (for $\tau = 0.01$), thus giving the appearance that increasing Sm_c is only destabilizing. It should be noted that most thermosolutal systems with τ of $O(0.01)$ have Sm_c and Sr_c values well below the above minimum value.

5. Eigenvectors and spatial structure at neutral stability

In this section the spatial structures of w, ϕ, χ, that underlie the neutral stability boundaries are briefly examined. Normalized eigenvectors of w, ϕ, χ for the basic state where $\Delta\bar{T}$ and $\Delta\bar{C}$ are imposed across the fluid layer are shown in figures 10 and 11, and the eigenvectors for a basic state where $\Delta\bar{C}$ is induced by $\Delta\bar{T}$ are shown in figure 12. The spatial shapes correspond to sets of parameter values on the stability boundaries presented in §4. For example, in figures 10 and 11 the eigenvectors associated with Ms_c values of -250, -500, -800 and -1000 correspond to points on oscillatory boundaries shown in figure 7. Similarly, in figure 12 the eigenvectors associated with Sm_c values of 0.01, 0.05 and 0.1 correspond to three points on the ($\tau = 0.01$) oscillatory stability in figure 4. In each of the nine graphs in figures 10–12, a single eigenvector is shown which represents the spatial structure of w, ϕ, χ at any point along the stationary neutral stability branches.

The w eigenvectors display the least variation, ϕ eigenvectors exhibit some variation and χ eigenvectors show the greatest sensitivity to changes in Ms_c or Sm_c. Closer inspection of figures 10(*a*), 11(*a*) and 12(*a*) reveals that the w eigenvectors are

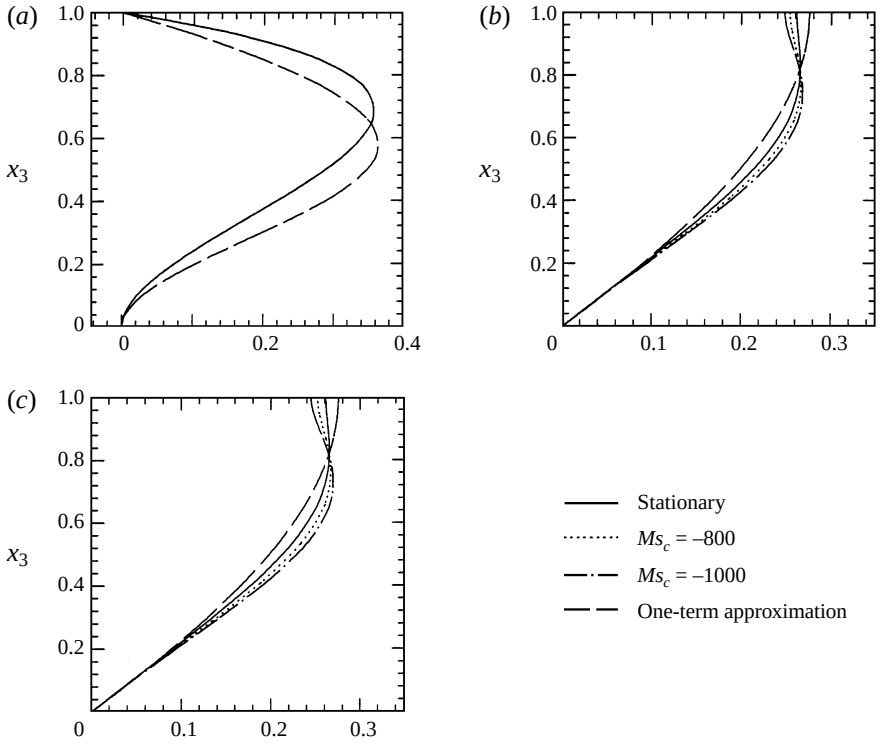

FIGURE 11. Velocity, temperature, and concentration eigenvector profiles at neutral stability. $\Delta\bar{T}$ and $\Delta\bar{C}$ both imposed across the layer. $Pr = 1800$, $\tau = 0.772$, $Sm = 0.072$, $Dm = 0.183$, $Nu = 0$, and $Sh = 0$. (*a*) Normalized velocity eigenvector vs. x_3. (*b*) Normalized temperature eigenvector vs. x_3. (*c*) Normalized concentration eigenvector vs. x_3.

essentially identical and invariant for all parameter values and basic states we explored. In all cases, the maximum normalized w value of 0.357 was obtained at $x_3 = 0.687$. For small Pr values typical of binary liquid metal alloys, we suspect that larger variations would be observed in w eigenvectors along the oscillatory branch. The behaviour of the ϕ eigenvectors approaches that of χ for the larger τ value, 0.772, of the ternary system (figures 11(*b*) and 11(*c*)).

The χ eigenvectors associated with oscillatory flow exhibit greater distortion and more severe spatial gradients owing to the small τ values than either the w or ϕ eigenvectors. The distortion and severity of the spatial gradients are also found to be larger for larger negative values of Ms_c or Sm_c. Therefore, the shape of χ, on the oscillatory stability branch, becomes more complicated further from the codimension two point (negative Ms_c values); as well as for decreasing τ values. The computational significance is that greater spatial resolution (or number of basis functions) of a given numerical scheme is required to extend the oscillatory stability boundary further from the codimension two point. Similarly, to obtain accuracy equivalent to larger $\tau(O(1))$, increased resolution is necessary for very small values of τ. Inspection of figures 10, 11 and 12 further suggests that the greatest impact on accuracy is achieved by adjusting the number of χ basis functions independent of w and ϕ.

Careful inspection reveals that the stationary normalized eigenvectors for w, ϕ, χ for each of the three cases shown in figures 10, 11 and 12 are identical. It can be shown from the exact solutions of w, ϕ, χ, that spatial shapes are affected only by α. Parameters, τ, Dm, Sm, Ma, Ms, Nu and Sh influence only the magnitudes of w, ϕ, χ

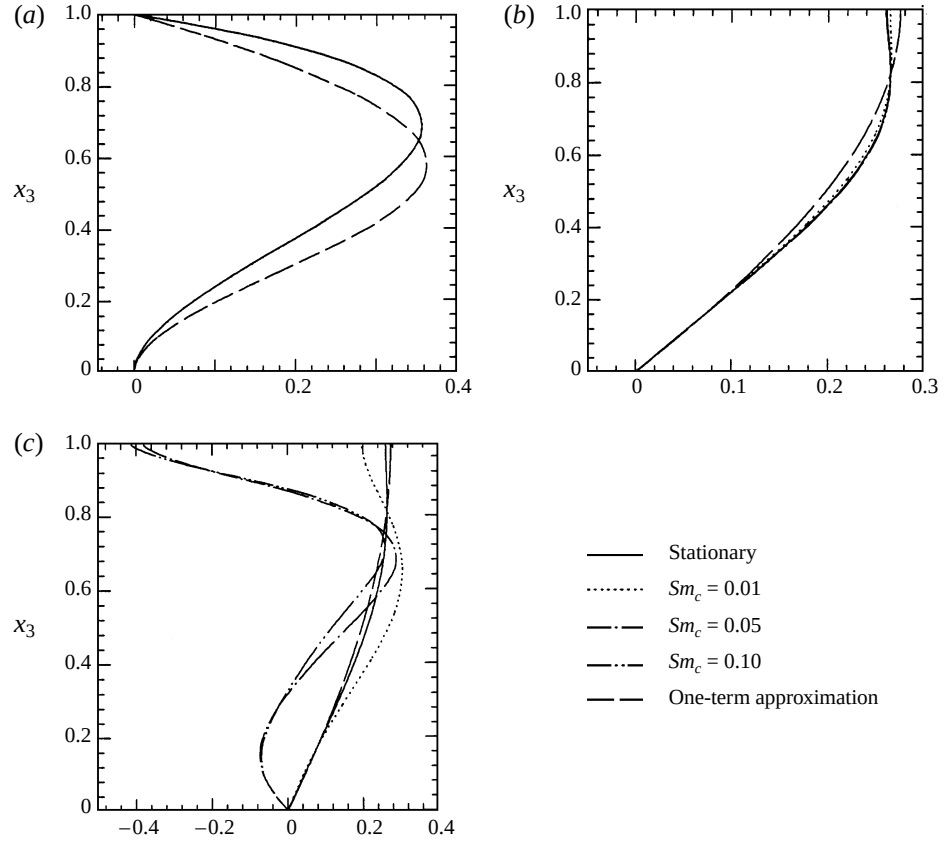

FIGURE 12. Velocity, temperature, and concentration eigenvector profiles at neutral stability. $\Delta\bar{C}$ induced by $\Delta\bar{T}$ across the layer. $Pr = 6.97$, $\tau = 0.0077$, $Sm = -0.028$, $Dm = 0$, $Nu = 0$, and $Sh = 0$. (*a*) Normalized velocity eigenvector vs. x_3. (*b*) Normalized temperature eigenvector vs. x_3. (*c*) Normalized concentration eigenvector vs. x_3.

(For stationary stability, τ plays no role when both $\Delta\bar{T}$ and $\Delta\bar{C}$ are imposed across the layer.) In general, α_c, hence the spatial solution shapes, vary along the stationary stability. However, as McTaggart (1983) concluded, when $Nu = Sh$, α_c is constant along the stationary neutral stability branch. This also follows in the presence of cross-diffusion, therefore the spatial shapes of w, ϕ, χ or normalized eigenvectors are invariant along the stationary stability boundary, i.e. independent of τ, Dm, Sm, Ma, and Ms. Furthermore, the stationary solution shapes of the two basic states we have studied are identical for an insulated and impermeable free surface (or whenever $Nu = Sh$).

6. One-term approximations

High-order weighted-residual-schemes provide high-accuracy solutions as demonstrated in §4; however, the required numerical output to examine the effects of several parameters is also large. An alternative approach is to develop one-term Galerkin formulations that yield algebraic expressions from which parametric effects might easily be examined. Such approaches are advocated in Finlayson's treatment of weighted residual methods (1972) and exploited during Gershuni & Zhukhovitskii's examination

of Rayleigh–Bénard type problems (1976). Algebraic relations that can be used to examine stability characteristics of the cross-doubly-diffusive-Marangoni fluid layer are developed using a one-term Galerkin formulation.

The one-term Galerkin formulation leads to an eigenvalue problem of the form:

$$\lambda \begin{bmatrix} b_1 & 0 & 0 \\ 0 & b_2 & 0 \\ 0 & 0 & b_3 \end{bmatrix} \begin{bmatrix} \hat{w} \\ \hat{\phi} \\ \hat{\chi} \end{bmatrix} = \begin{bmatrix} a_{11} & a_{12} & a_{13} \\ a_{21} & a_{22} & a_{23} \\ a_{31} & a_{32} & a_{33} \end{bmatrix} \begin{bmatrix} \hat{w} \\ \hat{\phi} \\ \hat{\chi} \end{bmatrix}. \tag{18}$$

The above system yields a cubic characteristic equation of the form, $\lambda^3 + c_2\lambda^2 + c_1\lambda + c_0 = 0$, where $\lambda = \rho + \mathrm{i}\omega$, ($\rho$ and ω are both real). Substituting the growth rate, ρ, and frequency, ω, in place of λ, the characteristic equation is expressed as the following two (real) equations (Gantmacher 1959).

$$\rho^3 + c_2(\rho^2 - \omega^2) - 3\rho\omega + c_1\rho + c_0 = 0, \tag{19}$$

$$-\omega^3 + 2c_2\omega\rho + 3\omega\rho^2 + c_1\omega = 0. \tag{20}$$

Stability characteristics of the resulting cubic system are assessed by applying the following criteria. Stationary stability occurs for $c_0 = 0$ while oscillatory stability occurs when $c_0 = c_1 c_2$, where $\omega^2 = c_1 > 0$ (Finlayson 1972; Gershuni & Zhukhovitskii 1976). Criteria to determine the location of the codimension two point can also be established.

When $\Delta\bar{T}$ and $\Delta\bar{C}$ are both imposed across the fluid layer, the matrix coefficients, b_i and a_{ij} are:

$$b_1 = [(D\hat{w}, D\hat{w}) + \alpha^2(\hat{w}, \hat{w})]/Pr \quad b_2 = (\hat{\phi}, \hat{\phi}) \quad b_2 = (\hat{\chi}, \hat{\chi})$$

$$a_{11} = -[(D^2\hat{w}, D^2\hat{w}) + 2\alpha^2(D\hat{w}, D\hat{w}) + \alpha^4(\hat{w}, \hat{w})] \quad a_{12} = -\alpha^2\hat{\phi}(1)\, D\hat{w}(1)$$

$$a_{13} = -\alpha^2\,\hat{\chi}(1)\, D\hat{w}(1) \quad a_{21} = Ma_1(\hat{w}, \hat{\phi}) \quad a_{22} = -(D\hat{\phi}, D\hat{\phi}) + \alpha^2(\hat{\phi}, \hat{\phi})$$

$$a_{23} = -Dm[(D\hat{\chi}, D\hat{\phi}) + \alpha^2(\hat{\chi}, \hat{\phi})] \quad a_{31} = Ma_2(\hat{w}, \hat{\chi}) \quad a_{32} = -Sm[(D\hat{\phi}, D\hat{\chi}) + \alpha^2(\hat{\phi}, \hat{\chi})]$$

$$a_{33} = -\tau[(D\hat{\chi}, D\hat{\chi}) + \alpha^2(\hat{\chi}, \hat{\chi})]$$

Where (f, g) is the inner product defined as:

$$(f, g) = \int_0^1 f(x_3)\, g(x_3)\, \mathrm{d}x_3.$$

The success of the one-term approximation rests on constructing a 'suitable' trial function. One rule of thumb in this regard is that the trial function explicitly satisfy the boundary conditions so that no error is introduced at the boundaries (Finlayson 1972). For this study, the velocity trial function, equation (21), was chosen to satisfy $w(0) = Dw(0) = w(1) = 0$, while the tangential stress conditions at $x_3 = 1$ is incorporated into the weak formulation of the momentum equation as a boundary residual. The temperature and concentration trial functions, equations (22) and (23), satisfy the conductive-permeable conditions at the $x_3 = 0$ and insulated-impermeable conditions at the free surface. Shapes of the trial functions are shown in figures 10, 11 and 12.

$$\hat{w}(x_3) = (1 - x_3)\, x_3^2 + \frac{1}{\pi^2}\sin^2(\pi x_3), \tag{21}$$

$$(\hat{\phi}(x_3), \hat{\chi}(x_3)) = (1 - \tfrac{1}{2}x_3)\, x_3 + \sin(\tfrac{1}{2}\pi\, x_3). \tag{22}$$

These trial functions result in the following approximate expressions for stationary stability, oscillatory stability, frequency, and the codimension two point.

Stationary stability, $c_0 = 0$

$$k_1 = \frac{(1-Sm)\,Ma + (1-Dm)\,Ms}{1-Sm\,Dm}, \tag{23}$$

Oscillatory stability, $c_0 = c_1 c_2$

$$Ma(1+\tau\,Sm) + \tau\,Ms(\tau+Dm) + k_5\,Pr(Ma+\tau\,Ms) = k_2\frac{\tau}{Pr}(1+\tau)(1-Sm\,Dm) + k_1(1+\tau^2) + k_3\,Pr(1+\tau) + k_4\tau, \tag{24}$$

Frequency, $\omega^2 = c_0/c_2$

$$\omega^2 = \frac{Pr\,\tau(k_1(1-Sm\,Dm) - (1-Sm)\,Ma - (1-Dm)\,Ms)}{k_6((1+\tau) + k_5\,Pr)}. \tag{25}$$

Codimension two point

$$Ms_{co2} = \frac{k_1\dfrac{1-Dm\,Sm}{1-Sm} - \dfrac{k_2\dfrac{\tau}{Pr}(1+\tau)(1-Sm\,Dm) + k_1(1+\tau^2) + k_3\,Pr(1+\tau) + k_4\tau}{1+\tau\,Sm+k_5\,Pr}}{\dfrac{1-Dm}{1-Sm} - \dfrac{\tau(\tau+Dm+k_5\,Pr}{1+\tau\,Sm+k_5\,Pr}}, \tag{26}$$

where: $k_1 = 71.55106$, $k_2 = 20.99734$, $k_3 = 243.8594$, $k_4 = 143.1141$, $k_5 = 3.40791$, $k_6 = 0.470219$.

When $\Delta\bar{C}$ is induced by an applied $\Delta\bar{T}$, equations (23)–(26) can be used by making the substitution, $Ms_c = -(Sm_c/\tau)\,Ma_c$. For stationary stability the result is:

$$Ma_c = \frac{k_1(1-Dm\,Sm)}{1-Sm+\dfrac{Sm}{\tau}-\dfrac{Dm\,Sm}{\tau}}. \tag{27}$$

The critical wavenumber was shown in figures 8 and 9 to be relatively insensitive to location along the oscillatory boundary for the set of boundary conditions imposed. Moreover, the α_c from the one-term approximation is even less sensitive, with variations of α_c being less than 0.1 % of α_{1c} for the range of values shown in figures 13(*a*) and 13(*b*). Therefore, the stationary critical wavenumber obtained from the one-term Galerkin approximation, $\alpha_{1c} = 2.05203$, was applied to determine the one-term relationships given by (23) to (26).

The accuracy of the one-term Galerkin formulae is examined in figures 13 and 14 for the case of $\Delta\bar{T}$ and $\Delta\bar{C}$ imposed across the fluid layer. The predicted stability boundaries are in good agreement with the higher-order results for both the thermosolutal and ternary systems shown in figures 13(*a*) and 13(*b*), respectively. One disagreement is that the oscillatory boundary predicted from the one-term formulation shows a stabilizing behaviour with decreasing Ms_c, while the spectral results show destabilization. Near Sm_{co2} and Ms_{co2} values, one-term computed frequencies show satisfactory agreement with the higher-order spectral predictions shown in figures 13(*b*) and 14(*b*). For the thermosolutal system, one-term predictions quickly diverge from the spectral solution with larger stabilizing Ms_c values, while, better agreement

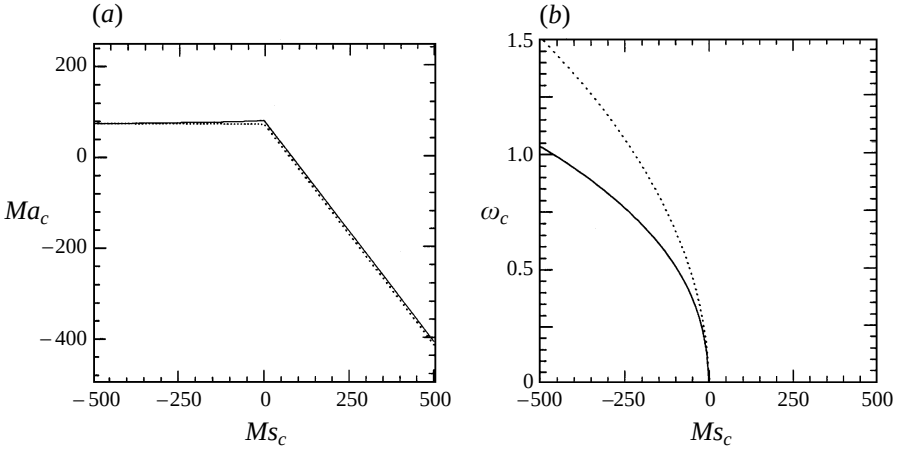

FIGURE 13. Comparison of stability boundaries computed from the ……, one-term Galerkin and ——, the higher-order spectral scheme ($n = 10$) for the thermosolutal system. $\Delta\bar{T}$ and $\Delta\bar{C}$ are both imposed across the layer. $Nu = 0$ and $Sh = 0$. (*a*) Ms_c vs. Ma_c for $Pr = 6.97$, $\tau = 0.0077$, $Sm = -0.0288$, $Dm = 0$. (*b*) Ms_c vs. ω_c for $Pr = 6.97$, $\tau = 0.0077$, $Sm = -0.0288$, $Dm = 0$.

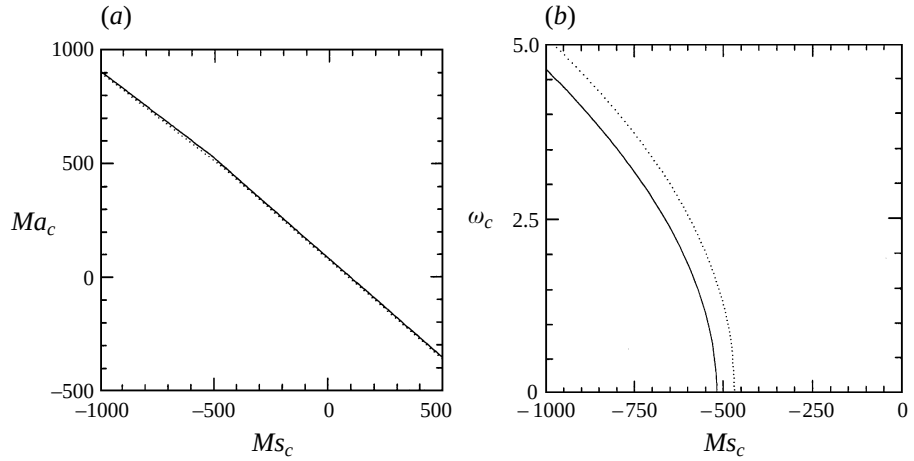

FIGURE 14. Comparison of stability boundaries computed from ……, the one-term Galerkin and ——, the higher-order spectral scheme ($n = 12$) for the ternary system. $\Delta\bar{T}$ and $\Delta\bar{C}$ are both imposed across the layer. $Nu = 0$ and $Sh = 0$. (*a*) Ms_c vs. Ma_c for $Pr = 1800$, $\tau = 0.772$, $Sm = 0.072$, and $Dm = 0.183$. (*b*) Ms_c vs. ω_c for $Pr = 1800$, $\tau = 0.772$, $Sm = 0.072$, and $Dm = 0.183$.

between the one-term Galerkin results and the spectral solution is observed for the ternary system. Codimension two-point locations predicted by (26) are shown in tables 1 and 2, and compare quite well with the higher-order predictions.

Similar conclusions hold true for the case of $\Delta\bar{C}$ induced by $\Delta\bar{T}$ from inspection of figure 15. The one-term stationary results are in excellent agreement with results from the exact solution. The critical values predicted from the one-term formulation are in good agreement with higher-order results. For $\tau = 0.01$, the oscillatory branch decreases with Sm_c for $Sm_c < 0.33$ and increases beyond this Sm_c value while the one-term Galerkin results show only the increase in Ma_c. At larger τ values ($\tau = 0.1$ shown in figure 15*a*) one-term results and higher-order spectral results both show a stabilizing influence with increasing Sm_c. Codimension two-point locations are found to compare quite well with the higher-order predictions in table 4.

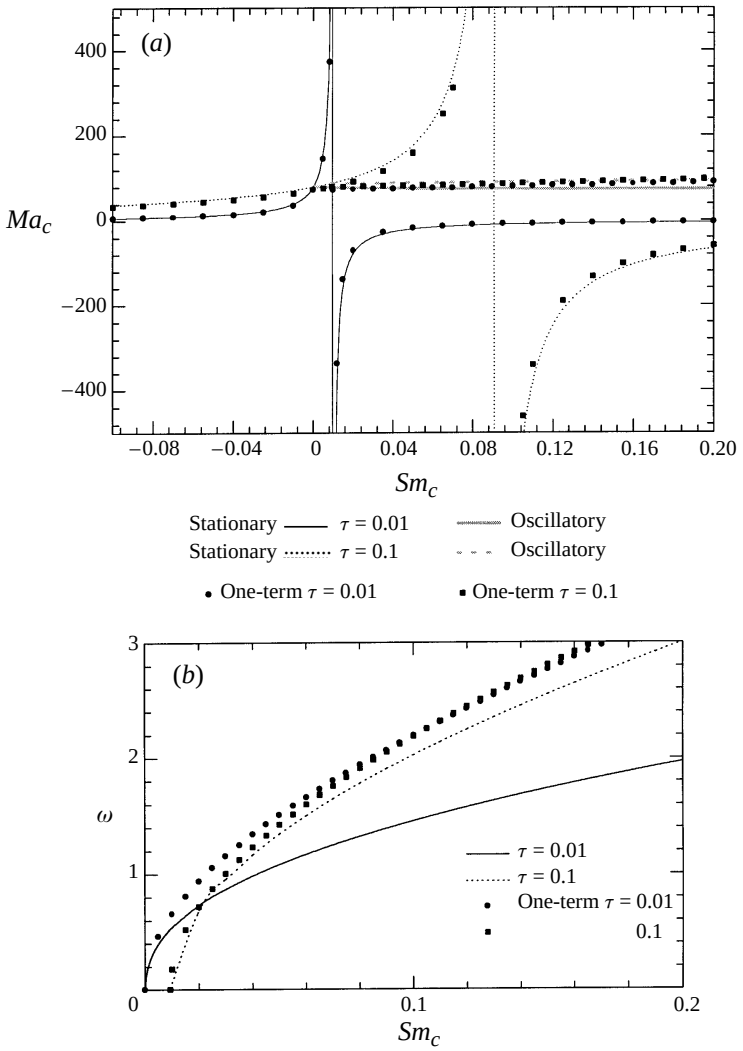

FIGURE 15. Comparison of stability boundaries computed from the one-term Galerkin and the higher-order spectral scheme for the thermosolutal system. $\Delta\bar{C}$ induced by $\Delta\bar{T}$; $Nu = 0$ and $Sh = 0$. (*a*) Sm_c vs. Ma_c for $Pr = 6.97$, $Sm = -0.288$, $Dm = 0$ for τ values of 0.01 and 0.1. (*b*) Sm_c vs. ω_c for $Pr = 6.97$, $Sm = -0.0288$, $Dm = 0$ for τ values of 0.01 and 0.1.

The one-term derived relationship, (26), provides reasonable estimates of the codimension two-point location as a function of Ms_c, Ma_c, Sm_c, τ and Pr. The alternative is full numerical simulations for several sets of parameter values. As noted in previous studies (Chen & Chen 1994; Ho & Chang 1988) determining the codimension two point is generally very time-consuming. It is interesting that the asymptote predicted from (27) has the exact location obtained from the exact solution.

7. Summary and conclusions

We investigated linear stability of the cross-doubly-diffusive Marangoni instability for two different basic states. The first basic state is one where both $\Delta\bar{T}$ and $\Delta\bar{C}$ are imposed across the layer, while the second case is a basic state where the imposed $\Delta\bar{T}$

across the layer induces a $\Delta\bar{C}$. Rather than adopting and extending reference quantities from the buoyancy problem, our reference quantities were explicitly defined to attack onset of convection driven by surface-tension variation in the zero gravity limit. This led to the definition of a surface tension Soret coefficient and a surface tension Dufour coefficient which function analogously to their buoyancy counterparts. The scaling leads to a concise description of results in the zero gravity limit. The introduction of buoyancy does require an additional parameter that relates buoyancy and surface-tension properties (Chen & Chen 1994).

While retaining both cross-diffusion terms and general disturbance heat and mass flux conditions at the free surface, exact solutions for stationary stability were obtained for both basic states. The location of asymptotes in relevant parameter space were also determined from exact solutions. For an insulated and impermeable free surface, we found that exact asymptote location was expressed in the form identical to an exact asymptote relation derived for the buoyancy-driven problem, (Hurle & Jakeman 1971). Furthermore, when τ is small, as is the case for water–alcohol mixtures and liquid metal alloys, the asymptote location, Sm_∞, is approximated well by $Sm_\infty \approx \tau$. The disturbance flux parameters, Nu and Sh, also affect the location of the stationary stability asymptotes as well as overall stability behaviour. The wavenumber, α_c, is profoundly influenced by the disturbance heat flux conditions, and in principal can be forced to any value in the range $0 \leqslant \alpha_c \leqslant \infty$, for appropriate values of Nu and Sh.

One interesting distinction between the two basic states is the effect of τ. For $\Delta\bar{C}$ and $\Delta\bar{T}$ both imposed across the layer, stationary stability is independent of τ. In contrast, for the case where $\Delta\bar{C}$ is induced, increasing τ has a stabilizing effect on stationary stability in (Sm_c, Ma_c) space. Increasing τ was also found to stabilize the time-dependent stability boundaries for both basic states investigated.

When both $\Delta\bar{T}$ and $\Delta\bar{C}$ are imposed and for small τ, the oscillatory branch in (Ma_c, Ms_c) space decreases with increasingly stable concentration gradients (negative Ms_c). This decrease of the oscillatory branch away from the codimension two point was also observed for the double-diffusive problem in the absence of cross-diffusion. Although this behaviour has not been reported in previous double diffusive linear stability papers, an energy stability study by Castillo & Velarde (1982) also shows decreasing Ma_c with increasingly negative Ms_c in the oscillatory regime.

Results obtained from the one-term Galerkin formulation qualitatively reflect the stability behaviour predicted from the higher-order approximations. A practical consequence is that the nature of the stability can be determined approximately, without solving the numerical eigenvalue problem. Another benefit of the one-term derived relationships of this study is a reliable estimate of the codimension two points. It was also surprising to find that the stationary state asymptote (for induced $\Delta\bar{C}$) predicted from the one-term formulation is identically the exact solution. Buoyancy was not considered as part of the investigation; however, the one-term expressions could easily be extended to accommodate the combined effects of buoyancy and surface tension. Moreover, the extended one-term approximations would allow rapid and convenient estimation of stability behaviour for the combined systems.

The first author thanks Professor N. Fitzmaurice for initial guidance with implementation of collocation schemes. This work was performed as part of NASA's Microgravity Fluid Physics Program and supported by NASA's Microgravity Sciences Division.

REFERENCES

Adamson, A. W. 1982 *Physical Chemistry of Surfaces*, 4th edn. John Wiley.

Castillo, J. L. & Velarde, M. G. 1978 Thermal diffusion and the Marangoni–Bénard instability of a two-component fluid layer heated from below. *Phys. Lett.* **66**A, 489–491.

Chandrasekhar, S. 1981 *Hydrodynamic and Hydromagnetic Stability*. Dover.

Chen, C. F. & Chen, C. C. 1994 Effect of surface tension on the stability of a binary fluid layer under reduced gravity. *Phys. Fluids* **6**, 1482–1490.

Cussler, E. L. 1995 *Diffusion Mass Transfer in Fluid Systems*. Cambridge University Press.

Davis, S. H. 1987 Thermocapillary instabilities. *Ann Rev. Fluid Mech.* **19**, 403–435.

Finlayson, B. A. 1972 *The Method of Weighted Residuals and Variational Principles with Application in Fluid Mechanics, Heat and Mass Transport*. Academic.

Gantmacher, F. R. 1959 *Matrix Theory*. Chelsea.

Gershuni, G. Z. & Zhukhovitskii, E. M. 1976 *Convective Stability of Incompressible Fluids*. Keter, Jerusalem.

Henry, D. 1990 Analysis of convection situations with Soret effect. In *Low-Gravity Fluid Dynamics and Transport Phenomenon* (ed. J. N. Coster & R. L. San). Progress in Astronautics and Aeronautics.

Henry, D. & Roux, B. 1988 Soret separation in a quasi-vertical cylinder. *J. Fluid Mech.* **195**, 175–200.

Ho, K. L. & Chang, H. C. 1988 On nonlinear doubly-diffusive Marangoni instability. *AIChE J.* **34**, 705–722.

Hurle, D. T. & Jakeman, E. 1969 Significance of the Soret effect in the Rayleigh–Jeffery's problem. *Phys. Fluids* **12**, 2704–2705.

Hurle, D. T. & Jakeman, E. 1971 Soret-driven thermosolutal convection. *J. Fluid Mech.* **47**, 667–687.

Jacqmin, D. 1990 Parallel flows with Soret effect in tilted cylinders. *J. Fluid Mech.* **211**, 355–372.

Legros, J. C., Dupont, O., Queeckers, P., Van Vaerenbergh, S. & Schwabe, D. 1990 Thermohydrodynamic instabilities and capillary flows. In *Low-Gravity Fluid Dynamics and Transport Phenomenon* (ed. J. N. Coster & R. L. Sani). Progress in Astronautics and Aeronautics.

McDougall, T. J. 1983 Double-diffusive convection caused by coupled molecular diffusion. *J. Fluid Mech.* **126**, 379–397.

McTaggart, C. L. 1983 Convection drive by concentration- and temperature-dependent surface tension. *J. Fluid Mech.* **134**, 301–310.

Pearson, J. R. A. 1958 On convection cells induced by surface tension. *J. Fluid Mech.* **4**, 489–500.

Platten, J. K. & Chavepeyer, G. 1973 Oscillatory motion in a Bénard cell due to the Soret effect. *J. Fluid Mech.* **60**, 305–319.

Stern, M. E. 1960 The salt-fountain and thermohaline convection. *Tellus* **12**, 599–611.

Torrones, G. & Chen, C. F. 1993 Convective stability of gravity-modulated doubly cross-diffusive fluid layers. *J. Fluids Mech.* **225**, 301–321.

Turner, J. S. 1973 *Buoyancy Effects in Fluids*. Cambridge University Press.

Velarde, M. G. & Castillo, J. L. 1982 Transport and reactive phenomenon leading to interfacial instability. In *Convective Transport and Instability Phenomena* (ed. J. Zierep & H. G. Oertel). G. Braun.